If the terms including $K\Gamma_0$ in the numerator and denominator are neglected, R is approximated by

$$R=\Gamma_0 N D\pi^{3/2}\frac{\lambda^2}{\Delta_i}g\left(\frac{1+f}{2+f}\right)^{1/2}\exp\left[-\frac{f\delta^2}{(2+f)(1+f)\Delta_e^2}\right]. \quad \text{(A12)}$$

The solution of (A12) gives a first approximation to Γ_0, which can be solved from Eq. (A11) using an iterative technique.

PHYSICAL REVIEW VOLUME 133, NUMBER 3B 10 FEBRUARY 1964

Reactions Induced in Fe^{54} with 21–63 MeV Li^6 Ions*

MARSHALL BLANN, FRANK M. LANZAFAME, AND R. AMELIA PISCITELLI
Department of Chemistry, University of Rochester, Rochester, New York

(Received 25 September 1963)

Excitation functions have been measured for the production of Ni^{56}, Ni^{57}, Co^{55}, Co^{56}, Co^{57}, Co^{58}, Fe^{52}, Fe^{55}, and Mn^{54} from Fe^{54} bombarded with Li^6 ions of 21–63-MeV kinetic energy. The targets were enriched to 95% Fe^{54}. Excitation functions for the production of Ni^{57}, Co^{55}, Co^{56}, Co^{57}, Fe^{55}, and Mn^{54} resulting from Li^6 bombardment of Fe^{54} and deuteron bombardment of Ni^{58} are compared. Of these, excitation functions for the production of Ni^{57}, Co^{57}, and Mn^{54} are mutually consistent with decay of a Cu^{60} compound nucleus. Excitation functions for production of Co^{55} and Fe^{55} with the two projectiles appear to proceed by different mechanisms. The Co^{56} excitation functions in the two target-projectile systems are not directly comparable, since the probable reactions producing Co^{56} are $Ni^{58}(d,\alpha)Co^{56}$ and $Fe^{54}(Li^6,2p2n)Co^{56}$. All excitation functions studied in the $Fe^{54}+Li^6$ system show the competitive behavior of compound-nucleus reactions with the exception of the high-energy tail of the Co^{58} excitation function (apparently due to 5% Fe^{56} impurity in the targets) and the low-energy portions of the Co^{55} and Fe^{55} excitation functions. The very low yields observed for the production of Ni^{56} and Ni^{57} are attributed to the effect of the 28-nucleon shells on nuclear level densities. The sum of measured cross sections from $Fe^{54}+Li^6$ reactions is compared with calculated optical-model nonelastic cross sections.

I. INTRODUCTION

THE present work describes experimental results of measurements of excitation functions resulting from the Li^6 bombardment of Fe^{54}. The investigation was undertaken as part of a general study of the compound-nucleus reaction mechanism, with particular interest in the applicability of statistical theory to the decay of the compound nucleus. Reactions at intermediate energies are, in general, mixtures of direct interaction and compound-nucleus processes. It is meaningless to compare predictions of the statistical theory with experimental results corresponding to direct interactions. For this reason one must first have at least qualitative evidence that a given set of reactions proceeds predominantly by the compound-nucleus mechanism before applying statistical mechanics for a theoretical prediction of decay products. To provide such qualitative evidence was the general motivation for undertaking this work.

The system selected for this study ($Fe^{54}+Li^6$) was chosen for several reasons. First, the compound nucleus formed (assuming one is formed) is Cu^{60}, which is the same compound nucleus formed with deuterons incident on Ni^{58}. The yields of reaction products formed in the $Ni^{58}+d$ system were shown to be fairly consistent with formation from the decay of a compound nucleus at statistical equilibrium.[1] The highest excitation energy produced with deuterons on Ni^{58} corresponds roughly to the lowest excitation energy produced with Li^6 ions on Fe^{54} in this work. Both systems have approximately the same average angular momentum in the overlapping region as well. Hence, if the relative yields of the decay products are the same for both systems in this region, there is additional evidence for considering both reactions as proceeding through a compound-nucleus mechanism. The $Fe^{54}+Li^6$ system may then be studied at higher excitations (and with higher angular momentum) than the $Ni^{58}+d$ system, since Li^6 ions of up to 63 MeV are available. One may then see if these reactions appear to be proceeding by the compound-nucleus mechanism to the highest excitations measured, and if so, determine whether or not the results are consistent with decay of a compound nucleus at statistical equilibrium.

Additional interest in study of reactions in this region lies in the relatively low yields of Ni^{56} and Ni^{57} with

* This work supported by the U. S. Atomic Energy Commission.

[1] M. Blann and G. Merkel, Phys. Rev. **131**, 764 (1963).

TABLE I. Experimental cross sections measured in this work, target thicknesses, and assumed nonelastic cross sections as a function of excitation energy.

Mean excitation energy (MeV)[a]	Target thickness mg/cm²	Assumed total nonelastic cross section (b)	Cross sections (mb) for production of: Ni^{56}	Ni^{57}	Co^{55}	Co^{56}	Co^{57}	Co^{58}	Fe^{55}	Fe^{52}	Mn^{54}
70.4±0.4	2.98	1.12	2.7	8	80	162	60	26	237	0.65	78
67.0±0.2	1.80	1.10	3.6	11	76	190	79	38	167	0.49	81
63.5±0.4	3.21	1.08	4.0	15	83	233	113	51	142	0.20	76
59.9±0.5	3.38	1.05	3.3	30	61	222	136	46	86		85
55.6±0.5	3.10	1.02	2.7	47	85	207	256	85	106		170
51.5±0.7	3.46	0.98	0.71	65	90	142	363	34	98		135
46.4±0.6	2.64	0.85		73	113	73	486	38	174		92
41.8±0.9	3.46	0.75		62	122	17	387	53	162		8
36.9±0.9	3.28	0.57		31	127		231	88	160		
34.7±0.2	0.70	0.41		6.0							

[a] The ± deviations expressed indicate the Li^6 energy spread through each target foil; the average excitation is listed. No estimate of straggling is included in the listed deviations. Range-energy values used are discussed in the text. Listed excitation energies were calculated assuming compound-nucleus formation.

respect to Co^{56} and Co^{57}.[2–7] It has been suggested that this anomaly is due to the effects of the 28-nucleon closed shell on level densities.[3,5] In the case of Ni^{58} $(\alpha,\alpha' xpyn)$ reactions it has also been suggested that the low yields may in part be due to the reactions proceeding by a direct (α,α') inelastic scattering process.[2] The production of cobalt isotopes would be favored in such a case since the proton binding energy is considerably less than the neutron binding energy in this region, hence a nucleus at low excitation would preferentially emit protons. In the $Fe^{54}+Li^6$ system one cannot produce Ni^{56} and Ni^{57} from inelastic scattering, and so one hopes to get unambiguous information on the effects of closed shells on level densities.

A final point of interest centers on the high-energy tail of the $Ni^{58}(d,\alpha)Co^{56}$ excitation function. While a direct process is a likely cause,[1] it is also possible that gamma-ray de-excitation may successfully compete with further particle emission after an alpha particle has been evaporated. If the $Fe^{54}(Li^6,\alpha)Co^{56}$ reaction does not exhibit the high-energy tail of the $Ni^{58}(d,\alpha)Co^{56}$ reaction, we would suspect that the latter tail results from a direct reaction rather than from a compound-nucleus $Ni^{58}(d,\alpha\gamma)Co^{56}$ reaction.

In this work we try to see which of the reactions studied proceed by the compound-nucleus mechanism, and which appear to be direct interactions. In a following paper,[8] one of the authors has applied the statistical theory to those excitation functions consistent with a compound-nucleus mechanism to see if the experimental results are consistent with the assumption of statistical equilibrium, to see what effect high angular momentum has on the reaction threshold and level densities, and to see if the 28-nucleon shell does indeed influence the nuclear level densities at high excitation energies.

II. EXPERIMENTAL PROCEDURES

A. Targets

Targets were made by electroplating enriched Fe^{54}(95.06±0.05% Fe^{54}, 4.84% Fe^{56}, 0.07% Fe^{57})[9] onto 0.2-mil gold foil. Gold foils one inch square were individually cut, measured, and weighed. Thicknesses varied between 10.2 and 10.9 mg/cm². Gold foil was the cathode in a plating chimney with a circular platinum anode. The anode was parallel to, and approximately one centimeter above, the cathode. The plating solution for each target consisted of 10 mg Fe^{3+}, 30 mg sodium tartrate, and an excess of 6N NH_4OH. Total volume was approximately 3 ml. It was possible to get smooth, adherent, and quantitative plates in one hour using two 1.5 V dry cells in series as power source. The actual thickness of each target used in this work is listed in Table I. The bombarded target stack consisted of 2.02-mg/cm² Al catcher-degrader foils interspersed between the target foils. A 5.17-mg/cm² Al foil enclosed the entire foil stack. The iron targets faced away from the beam in all but the last foil. The actual arrangement of target and catcher foils used is shown in Fig. 1.

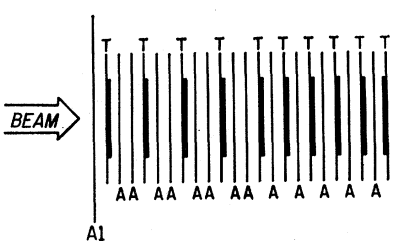

FIG. 1. Sequence of target and degrader foils used in target stack. Al=5.17 mg/cm² aluminum foil; T=Target foils, thicknesses listed in Table I; A=2.02 mg/cm² aluminum catcher-degrader foils.

[2] F. S. Houck and J. M. Miller, Phys. Rev. **123**, 231 (1961).
[3] M. Blann and G. Merkel, Nucl. Phys. (to be published).
[4] S. Tanaka, J. Phys. Soc. Japan **15**, 2159 (1960).
[5] R. A. Sharp, R. M. Diamond, and G. Wilkinson, Phys. Rev. **101**, 1493 (1956).
[6] S. R. Kaufman, Phys. Rev. **117**, 1532 (1960).
[7] H. A. Ewart (unpublished data).
[8] M. Blann, Phys. Rev. **133**, B707 (1964), following paper.
[9] Purchased from Oak Ridge National Laboratory.

TABLE II. Assumed half-lives, radiation type, and abundance for isotopes studies in this work.[a]

Nuclide	Type of radiation observed	Energy of radiation observed (MeV)	Assumed abundance	Assumed half-life
Ni^{56}	γ	0.164	0.99	6.1 day[b]
Ni^{57}	β^+		0.50	36.0 h
Co^{55}	β^+		0.60	18.2 h
Co^{56}	γ	1.26	0.70	77 day
Co^{57}	γ	0.120	1.00	270 day
Co^{58}	γ	0.810	1.00	71 day[c]
Fe^{52}	γ	0.163	1.00	8.3 h
	β^+		1.56	
Fe^{55}	K x ray	0.0059	0.28	2.6 yr[d]

[a] D. Strominger, J. M. Hollander, and G. T. Seaborg, Rev. Mod. Phys. 30, 585 (1958), unless otherwise referenced.
[b] D. O. Wells, S. L. Blatt, and W. E. Meyerhof, Phys. Rev. 130, 1961 (1963).
[c] The 0.810-MeV photopeak area represented yield of Co^{56} and Co^{58}. The fraction of the peak due to Co^{56} was calculated from the area of the 1.26-MeV peak and subtracted from the total 0.810-MeV peak area to obtain the Co^{58} contribution.
[d] C. D. Broyles, D. A. Thomas, and S. K. Haynes, Phys. Rev. 89, 715 (1953).

B. Bombardment

The target foil stack was bombarded with 63.0-MeV Li^6 ions (+3 charge state) at the Yale University heavy-ion linear accelerator. The beam passed through analyzing and 30° magnets before striking the target stack. The target holder, which was the Faraday cup, was connected to a calibrated Cary electrometer charge integrator which indicated a total beam current of 0.093 μA h in 57 min. Beam energy as a function of target depth was calculated using semiempirical ranges of Li^6 ions in aluminum[10] and the proton range data of Barkas,[11] for ranges in iron and gold. The proton ranges were converted to Li^6 ion range values by use of the relation[12]

$$R_{z,M,E}=(M/z^2)R_{P,E/M}.$$

C. Chemical Separations

The iron was dissolved from the gold foils with 16M HNO_3. The catcher foils were dissolved in the resulting nitric acid solution. Carriers of Ni, Co, and Mn were added, the solution was evaporated to dryness, and the nitrates were then converted to chlorides with 12M HCl. The chlorides were then dissolved in several ml of distilled water, and an excess of 10M NaOH was added. This precipitated hydroxides of Fe, Mn, Ni, and Co, and allowed separation of sodium aluminate. The hydroxides were dissolved in fuming HNO_3, and $KClO_3$ crystals were added to precipitate MnO_2. The supernatant was made basic with NaOH, the resulting hydroxides of Ni, Co, and Fe were dissolved in HCl, and a standard anion exchange procedure was used to separate Ni, Co, and Fe.[13] Precipitates were mounted on fiberglass filter papers and covered with 0.1-mil rubber hydrochloride. The chemical forms used for precipitation were nickel-dimethylglyoxime, potassium cobaltinitrite, iron 8-hydroxyquinolate, and manganese dioxide.

D. Disintegration Rate Determinations

The radiation detected for each isotope studied is summarized in Table II. Calibrated end window proportional counters were used for all measurements of β^+ radiation.[14,15] A 3-in.×3-in. NaI crystal and 512-channel pulse-height analyzer were used for x-ray measurement; the efficiency curves of Heath were used to obtain crystal efficiencies.[16] The Fe^{55} K x-rays were counted with a 1-in.-diam by $\frac{1}{32}$-in.-thick NaI crystal having a 3-mil-thick beryllium window. A geometric factor of 0.30 was calculated for the system. Corrections were applied for self-absorption and window absorption.

The cross sections measured in this work are listed in Table I; corrections for decay and parent-daughter relationships have of course been applied. Absolute values quoted are thought to be accurate to ±25% with the exception of the cross sections for the production of Co^{58}, Fe^{52}, and Fe^{55}. The Co^{58} cross sections are considered less certain than others because the γ-ray activity measured was the difference of two numbers of approximately equal size. The Fe^{52} cross sections are less certain due to poor counting statistics resulting from the small cross sections and long time (24 h) from end of bombardment to the start of counting. The Fe^{55} cross sections are thought to be less accurate due to poor counting statistics and the difficulty of observing

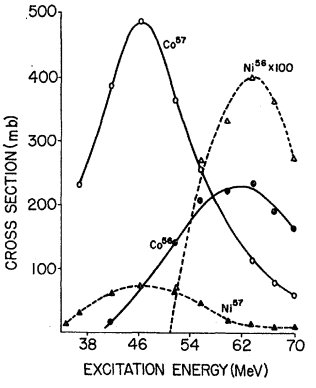

FIG. 2. Experimentally determined excitation functions for the production of Co^{56}, Co^{57}, Ni^{56}, and Ni^{57} from Fe^{54} bombarded with Li^6 ions. The Ni^{56} yields are plotted ×100.

[10] L. C. Northcliffe (unpublished).
[11] W. H. Barkas, Lawrence Radiation Laboratory Report UCRL-10292, 1962 (unpublished).
[12] G. Friedlander and J. W. Kennedy, *Nuclear and Radiochemistry* (John Wiley & Sons, Inc., New York, 1955), 2nd ed., Chap. 7, p. 194.
[13] B. G. Harvey, *Introduction to Nuclear Physics and Chemistry* (Prentice-Hall, Inc., Englewood Cliffs, New Jersey, 1962), Chap. 15, p. 313.
[14] B. P. Bayhurst and R. J. Prestwood, Nucleonics 17, No. 3, 82 (1959).
[15] M. Blann, Lawrence Radiation Laboratory Report UCRL-9190, 1960, Appendix B (unpublished).
[16] R. L. Heath, Atomic Energy Commission Research and Development Report IDO-16408, 1957 (unpublished).

the soft K x rays. We believe the cross sections reported for Fe^{52}, Fe^{55}, and Co^{58} are correct to $\pm 50\%$ or better.

III. RESULTS AND DISCUSSION

The excitation functions for the production of Co^{57}, Ni^{57}, Co^{56}, and Ni^{56} are presented in Fig. 2. These excitation functions show the competitive behavior characteristics of compound-nucleus reactions.[17,18] The Ni^{57} and Ni^{56} yields are considerably less than the Co^{57} and Co^{56} yields (note that the Ni^{56} excitation function is plotted $\times 100$) as has also been noted in $Ni^{58}(\alpha,\alpha' xpyn)$ reactions,[6,7] and in $Co^{59}(p,xpyn)$ reactions.[5] In this region of nuclides, neutron binding energies are 3–6 MeV greater than corresponding proton binding energies.[19] One might therefore expect that the relatively low yields of Ni^{56} and Ni^{57} may be explained solely on the basis of lower residual excitation energies in nickel isotopes producing correspondingly lower level densities, hence leading to lower yields. A statistical model analysis of the $Ni^{58}(\alpha,\alpha' xpyn)$ reactions shows that this effect is indeed present, but that it is not nearly adequate to account for the anomalously low nickel yields.[3] A more plausible explanation appears to be an additional decrease in nuclear level densities due to the 28-neutron and -proton shells. This effect has of course been predicted on theoretical grounds,[20–22] but experimental verification has been mainly in the region of the 50-proton shell.[23] Sharp *et al.* have suggested the effect is present in the region of the 28-nucleon shell; their evidence is based on $Co^{59}(p,xpyn)$ reaction yields.[5] Present experimental evidence for this shell effect is more abundant.[2–8]

Direct comparison of cross sections for the deuteron and lithium-ion-induced reactions would be meaningless, since at lower excitation energies in the Li^6+Fe^{54} system one is measuring a decrease in cross sections due to the Coulomb barrier. This may correspond to either an actual increase or decrease in emission probability leading to a given product. A more meaningful display results from dividing each measured cross section by the total compound-nucleus cross section corresponding to the kinetic energy of the incident ion leading to the measured cross section. Unfortunately, total compound-nucleus cross sections are unknown entities, and so we have used total nonelastic cross sections for deuterons on nickel and for lithium ions on iron, as calculated using the nuclear optical model.[24] The nonelastic cross section will include the contributions of direct interactions; we nonetheless assume they will be roughly proportional to the compound-nucleus cross sections in the region from the Coulomb barrier upward. The optical-model parameters used were the same for deuterons and lithium ions: $V=50$ MeV, $W=20$ MeV, $a=b=0.50$ F, and $R=(1.14A^{1/3}+1.20)$ F.[25] Volume absorption was assumed; spin-orbit interaction was assumed to be zero. The total nonelastic cross section versus lithium-ion kinetic energy is shown in Fig. 3 for the parameters listed above, as is a second calculated curve using the same parameters except that the lithium-ion particle size has been increased from 1.20 to 2.24 F. Comparison of the two curves of Fig. 3 from 21- to 63-MeV lithium-ion energy shows the percentage change in nonelastic cross section is not, fortunately, a particularly critical function of choice of radius parameters. The same statement is true in the calculations of deuteron nonelastic cross sections.

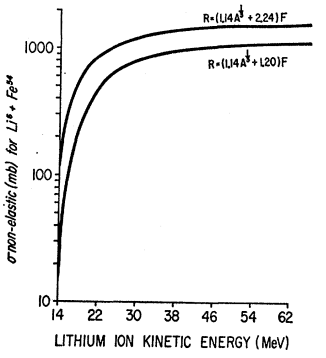

FIG. 3. Optical-model nonelastic cross sections versus kinetic energy for Li^6 ions incident on Fe^{54}. Optical-model parameters used are listed in the text. The lower curve was used for normalizing excitation functions of this work.

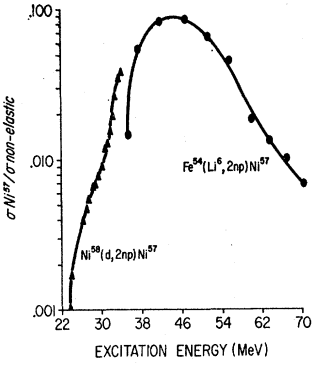

FIG. 4. Normalized excitation functions for the production of Ni^{57} from $Ni^{58}+d$ and $Fe^{54}+Li^6$. Triangles represent experimental yields from the deuteron-induced reactions of Ref. 1, circles represent values from the Li^6 ion-induced reactions.

The normalized cross sections ($\sigma_{\text{measured}}/\sigma_{\text{nonelastic}}$) for lithium-ion and deuteron-induced reactions are shown in Figs. 4–9. Normalized excitation functions for the production of Ni^{56}, Co^{58}, and Fe^{52} are shown in Fig. 10. The Ni^{56} and Fe^{52} excitation functions were not measured in the deuteron-induced reactions due to insufficient excitation available (24 MeV was the maximum deuteron kinetic energy). Cobalt-58 cross sections were not measured in the deuteron-induced reactions since

[17] V. F. Weisskopf, Phys. Rev. **52**, 295 (1937).
[18] S. N. Ghoshal, Phys. Rev. **80**, 939 (1950).
[19] F. Everling, L. A. Konig, J. H. E. Mattauch, and A. H. Wapstra, Nucl. Phys. **18**, 529 (1960).
[20] C. Bloch, Phys. Rev. **93**, 1086 (1954).
[21] N. Rosenzweig, Phys. Rev. **108**, 817 (1957).
[22] T. D. Newton, Can. J. Phys. **34**, 804 (1956).
[23] T. Ericson, in *Advances in Physics*, edited by N. F. Mott (Taylor and Francis, Ltd., London, 1960), Vol. 9, p. 425.
[24] The optical-model program used was due to F. E. Bjorklund and S. Fernbach.
[25] The parameters were chosen to be similar to published values for alpha particles as summarized in Ref. 1 of this work. The choice was arbitrary, but not overly critical.

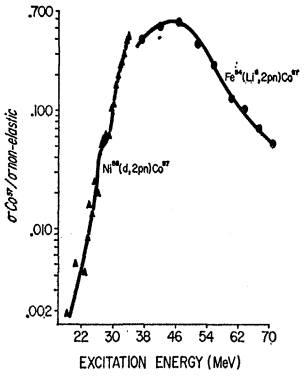

FIG. 5. Normalized excitation functions for the production of Co^{57} from $Ni^{58}+d$ and $Fe^{54}+Li^6$. Triangles represent experimental yields from the deuteron-induced reactions of Ref. 1, circles represent yields from the Li^6-induced reactions.

natural nickel was used as target, causing an ambiguity as to the mode of formation of Co^{58}, i.e., $Ni^{58}(d,2p)Co^{58}$ or $Ni^{60}(d,\alpha)Co^{58}$.

In the reactions investigated in this work, complex particles (d, t, He^3, and α) have a large emission probability. According to statistical theory, there are many permutations of sequence and aggregation state of emitted particles making significant contributions to the final products. For this reason we have simply abbreviated reactions by stating the total number of nucleons out, i.e., $(Li^6,2p2n)$, not meaning to imply that all nucleons necessarily are emitted singly. Exceptions to this convention are the reactions producing

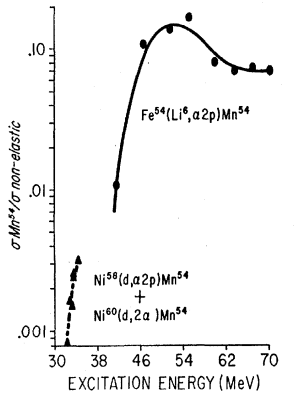

FIG. 6. Normalized excitation functions for the production of Mn^{54} from $Ni^{58,60}$ bombarded with deuterons and Fe^{54} bombarded with Li^6 ions. Triangles represent experimental yields from the deuteron-induced reactions of Ref. 1, circles represent yields from the Li^6-induced reactions.

Mn^{54} and Fe^{52} where energy considerations require that one of the emitted particles be an alpha particle.

Normalized excitation functions for the production of Ni^{57} and Co^{57} with both lithium ions and deuterons are shown in Figs. 4 and 5. While there is an apparent displacement of approximately 4 MeV to higher energies for the lithium-ion-induced reactions, this may well be within the uncertainty in the calculated range-energy curves used to calculate lithium-ion energy. Optical-model calculations indicate that both systems have approximately the same angular momentum distributions around 34 MeV of compound-nucleus excitation. A rotational energy shift would not, therefore, be a very plausible explanation for the discrepancy. Within the uncertainties of the range-energy curves, the two sets of reactions are consistent with a compound nucleus mechanism.

The normalized excitation functions for the production of Mn^{54} with lithium ions and deuterons are presented in Fig. 6. The comparison is of doubtful significance, since the mechanism of deuteron-produced Mn^{54} is uncertain, i.e., either from a $Ni^{58}(d,\alpha 2p)Mn^{54}$ reaction, or from a $Ni^{60}(d,2\alpha)Mn^{54}$ reaction. The strongest conclusion one can draw is that the two sets of curves are not inconsistent with a compound-nucleus mechanism. More definite conclusions could be reached for all the systems compared in this work if the deuteron-induced reactions were studied at higher energies. This investigation is now feasible with some of the new isochronous cyclotrons.

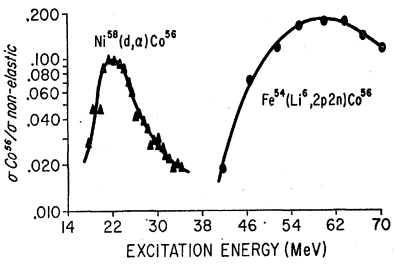

FIG. 7. Normalized excitation for the production of Co^{56} from $Ni^{58}+d$ and $Fe^{54}+Li^6$ ions. Triangles represent experimental yields from the deuteron induced reactions of Ref. 1, circles yield from the Li^6-induced reactions.

Figure 7 is a comparison of normalized excitation functions for the production of Co^{56} with lithium ions and deuterons. The former reaction apparently proceeds as an $Fe^{54}(Li^6,2p2n)Co^{56}$ reaction, while the latter reaction is apparently a $Ni^{58}(d,\alpha)Co^{56}$ reaction. The cross section for the production of Co^{56} with lithium ions is decreasing quite rapidly with decreasing excitation energy below 46 MeV. There was, in fact, insufficient activity to measure the cross section at 37 MeV of excitation. Failure to measure an $Fe^{54}(Li^6,2p2n)Co^{56}$ cross section in this region suggests that the tail on the $Ni^{58}(d,\alpha)Co^{56}$ excitation function arises from a direct process, rather than as a compound-nucleus (d,α) reaction.

Excitation functions for the production of Co^{55} and

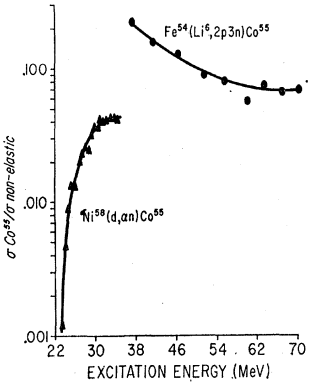

FIG. 8. Normalized excitation functions for the production of Co^{55} from $Ni^{58}+d$ and from $Fe^{54}+Li^6$ ions. Triangles represent experimental yields from the deuteron-induced reactions of Ref. 1, circles represent yields from the Li^6-induced reactions.

Fe^{55} with deuterons and lithium ions are presented in Figs. 8 and 9, respectively. The lithium-ion-induced reactions do not appear to be proceeding by a compound-nucleus mechanism, and in fact are probably proceeding through a single-particle stripping mechanism near and slightly above the Coulomb barrier, i.e., $Fe^{54}(Li^6,He^5)Co^{55}$ and $Fe^{54}(Li^6,Li^5)Fe^{55}$. Evidence for such a mechanism in heavy-ion-induced reactions has been presented by Wolfgang and his collaborators.[26]

Above 58 MeV of excitation the Fe^{55} excitation function shows a sudden increase. The onset of this increase coincides approximately with the decrease in four-particle-out excitation functions. It is likely that the increase is due to an $Fe^{54}(Li^6,3p2n)Fe^{55}$ compound-

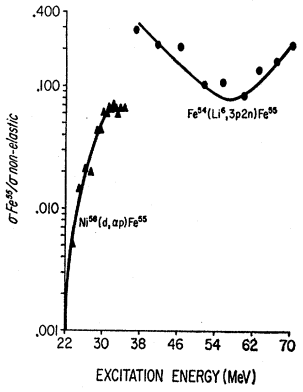

FIG. 9. Normalized excitation functions for the production of Fe^{55} from $Ni^{58}+d$ and from $Fe^{54}+Li^6$ ions. Triangles represent experimental yields from the deuteron-induced reactions of Ref. 1, circles represent yields from the Li^6-induced reactions.

nucleus reaction. The Co^{55} excitation function does not show as great an upturn as the Fe^{55} excitation function, and this could be due to the influence of the 28-neutron shell in Co^{55}. With such scant evidence this is of course purely speculative.

Excitation functions for the production of Co^{58}, Ni^{56}, and Fe^{52} are displayed in Fig. 10. The Co^{58} excitation function appears to be the result of the superposition of $Fe^{54}(Li^6,2p)Co^{58}$ and $Fe^{56}(Li^6,2p2n)Co^{58}$ compound-nucleus reactions. The "tail" of the Co^{58} excitation function has the same shape and position as the

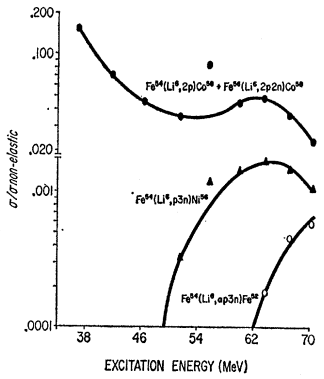

FIG. 10. Normalized excitation functions for the production of Co^{58}, Ni^{56}, and Fe^{52} from $Fe^{54}+Li^6$ ions. The Ni^{56} cross sections have been plotted $\times\frac{1}{2}$ to separate the Co^{58} and Ni^{56} excitation functions.

[26] J. B. J. Read, I. Ladenbauer-Bellis, and R. Wolfgang, Phys. Rev. **127**, 1722 (1962).

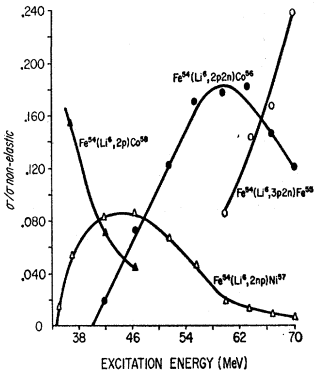

FIG. 11. Normalized excitation functions for the production of Co^{58}, Ni^{57}, Co^{56}, and Fe^{55} from $Fe^{54}+Li^6$ ions. Only the low-energy portion of the Co^{58} excitation function and the high-energy portion of the Fe^{55} excitation function are shown.

$Fe^{54}(Li^6,2p2n)Co^{56}$ and $Fe^{54}(Li^6,p3n)Ni^{56}$ excitation functions. Its magnitude as compared with that of the Co^{56} excitation function is roughly consistent with the 5% abundance of Fe^{56} in the targets. The sharp decrease in the Co^{58} excitation function at low excitation coincides with the increase of the three-nucleon-out excitation functions.

The Ni^{56} and Fe^{52} excitation functions also show the competitive behavior of compound nucleus reactions, the four-nucleon-out Ni^{56} excitation function increasing as the three-nucleon-out excitation functions decrease. The Ni^{56} yields in turn decrease as the five-particle-out Fe^{52} reaction becomes increasingly prominent.

The competitive nature of some of the reactions of this work is emphasized in Fig. 11, where the low-

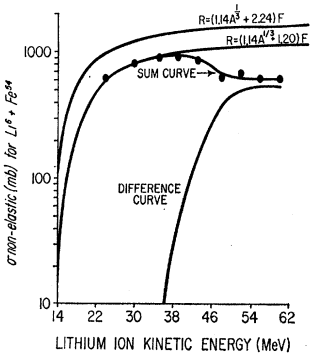

FIG. 12. Comparison of the calculated nonelastic cross sections for Li^6 ions incident on Fe^{54} with sums of experimental cross sections. Optical-model parameters used in calculating the nonelastic cross sections are listed in the text. A solid curve has been drawn through the points representing the sum of experimental yields. The lowest solid curve represents the difference between the lower nonelastic cross-section curve and the sum of experimental yields.

energy portion of the Co^{58} excitation function and the high-energy portion of the Fe^{55} excitation function are plotted along with the Ni^{57} and Co^{56} excitation functions. Figure 11 shows the effects of competition on two-, three-, and four-particle-out excitation functions. The Co^{57}, Ni^{56}, Mn^{54}, and Fe^{52} reactions also show this behavior.

The total reaction cross section is a separate, but interesting point. In Fig. 12 we have plotted the sum of experimentally measured cross sections from 37 to 70 MeV of excitation against the calculated nonelastic cross sections for Li^6 ions incident on Fe^{54}. Also shown

in Fig. 12 is the difference curve between the lower calculated curve and the experimental sum curve. The difference curve may probably be attributed to unmeasured five-particle-out reactions, such as the $Fe^{54}(Li^6,4pn)Mn^{55}$ reaction, to list but one possibility. The apparently excellent agreement between the experimental sum curve and the optical-model calculation is accidental since at all energies there are some unmeasured reactions. This implies that the lower calculated curve must be too low for the total nonelastic cross section, although it may be a good approximation to the compound-nucleus cross section.

IV. CONCLUSIONS

Of the reactions studied in this work, those producing Ni^{56}, Ni^{57}, Co^{56}, Co^{57}, Co^{58}, Mn^{54}, and Fe^{52} are consistent with the competitive behavior of compound-nucleus reactions.[17,18] Competition is shown from 36 to 70 MeV of excitation for reactions emitting two to five particles. Additional evidence for the compound-nucleus mechanism for the production of Ni^{57} and Co^{57} is obtained by comparison with $Ni^{58}(d,2pn)Co^{57}$ and $Ni^{58}(d,p2n)Ni^{57}$ excitation functions, where both the $Ni^{58}+d$ and $Fe^{54}+Li^6$ systems apparently form a Cu^{60} compound nucleus. The comparison of the two systems would be more complete and more meaningful if the deuteron-induced reaction measurements were extended to higher energy.

Reactions producing Co^{55} and Fe^{55} apparently proceed by a single-particle stripping mechanism at the lower lithium-ion energies; the excitation functions for these reactions bear little resemblance to the $Ni^{58}(d,\alpha n)Co^{55}$ and $Ni^{58}(d,\alpha p)Fe^{55}$ excitation functions. At the highest excitation energies studied, the $Fe^{54}(Li^6,3p2n)Fe^{55}$ reaction shows a rapid increase in probability, consistent with five-particle evaporation from a compound nucleus.

Comparison of cross sections for the production of Co^{56} and Co^{57} with those for the production of Ni^{56} and Ni^{57} shows very low yields for the nickel isotopes. A probable explanation for this lies in the influence of the 28-neutron and 28-proton closed shells on the level densities of singly magic Ni^{57} and doubly magic Ni^{56}.

Since the high-energy tail of the $Ni^{58}(d,\alpha)Co^{56}$ excitation function was not observed in the lithium-ion-induced reaction, we conclude that the (d,α) reaction is a direct reaction.

ACKNOWLEDGMENTS

The authors gratefully acknowledge Professor R. Wolfgang, Professor M. Kaplan, and Dr. I. Preiss for their help in scheduling the bombardment of this work on the Yale University heavy-ion accelerator, and for their hospitality at Yale University. We are similarly grateful to the operating crew of the accelerator for providing a record intensity lithium ion beam. We also express gratitude to L. Schwartz and J. Cooper for preparing the drawings of this work.